

§Electronic Supplementary Information (ESI)

Efficient encapsulation of functional proteins into erythrocytes by controlled shear-mediated membrane deformation

Md Habibur Rahman^{a,b,†}, Chung Hong N. Wong^{b,c,†}, Marianne M. Lee^{b,c}, Michael K. Chan^{b,c} and Yi-Ping Ho^{a,b,c,d,}*

^a Department of Biomedical Engineering, ^b Centre for Novel Biomaterials, ^c School of Life Sciences, ^d Hong Kong Branch of CAS Center for Excellence in Animal Evolution and Genetics, ^e The Ministry of Education Key Laboratory of Regeneration Medicine, The Chinese University of Hong Kong, Shatin, New Territories, Hong Kong SAR, China.

[†]These authors contributed equally to this work.

*Correspondent email: ypho@cuhk.edu.hk ; Tel: +852 3943 4340

ESI Text

Computational simulation model

The deformation of red blood cells (RBCs) was evaluated under steady laminar and laminar extension by COMSOL Multiphysics® v5.5 (Comsol Incorporation). The microfluidic channel was considered as a fluid domain and RBC was considered as a solid elastic material. Material parameters such as the Young's modulus ($E = 26$ KPa) and the Poisson's ratio ($\nu = 0.49$) of RBCs were obtained from previous studies¹. The fluid domain was solved by the Navier Stokes equation considering the conservation of momentum for incompressible fluid as denoted by²:

$$\rho \left(\frac{\partial u_{fluid}}{\partial t} + (u_{fluid} \cdot \nabla) u_{fluid} \right) = -\nabla \cdot P + F_{viscous} \quad (S1)$$
$$\rho \nabla \cdot u_{fluid} = 0$$

where, ρ is the fluid density, u_{fluid} is the fluid velocity, P is the fluid pressure, $F_{viscous}$ is the viscous force. No slip boundary conditions were assumed on the channel wall ($U_w = 0$) and zero velocity was assumed at the stagnation point. The deformation of RBC due to the stress imparted from the fluid motion was estimated by the Arbitrary Lagrangian-Eulerian (ALE) approximation using a fully coupled fluid solid interaction (FSI) module governed by the following equation²:

$$\rho_{solid} \frac{\partial^2 u_{solid}}{\partial t^2} = \nabla \cdot \sigma + F \quad (S2)$$

where, u_{solid} is the solid deformation, ρ_{solid} is the density of the solid material, σ is the stress components exerted on the linear elastic material from the fluid shear force F . The boundary of the elastic RBC has been considered freely floating in the fluid domain, therefore, the deformation of RBCs would be guided by the fluid motion. The mean shear stress (τ) was calculated (**Fig. 1B-C and [§]ESI Fig. S1B**) by the Newton's law of viscosity as shown below³:

$$\tau = \mu v \frac{4y}{h^2} \quad (S3)$$

where μ is the fluid viscosity, v is the fluid velocity, y and h are the width and height of the microchannel, respectively. The force field was obtained by integrating the shear stress exerted on the boundary of RBCs (**[§]ESI Fig. S2A-B**).

Fabrication of the microfluidic chip

Based on the stress estimation, the microchannel was designed with a uniform height of $40 \mu\text{m}$ to induce the mean shear stress within the range of 46 - 102 Pa around the cross-junction at the volumetric flow rate of 50 - $110 \mu\text{L}/\text{min}$. The microfluidic chips were fabricated following the standard soft lithography process.⁴ Briefly, a negative photoresist of SU8-2075 (Kayaku Advanced Materials) was spun on a 4" silicon wafer at $5,000$ RPM for 30 s to obtain the master mold of $40 \mu\text{m}$ height. The photoresist coated wafer was then exposed under UV (ABM-USA) through a Cr/Au mask (Microcad Photo-Mask Ltd). The developing and baking procedures of SU8-2075 were conducted following the manufacturer's datasheet. On the other hand, the microfluidic channel designed for the measurement of deformability index was patterned by a positive photoresist AZ 4620 to obtain a channel height of $5 \mu\text{m}$. The fabricated molds were hard baked at 180°C for 3 hr, followed by a surface modification using Trichloro(1H,1H,2H,2H-perfluorooctyl)silane (Sigma Aldrich, catalog no. 448931) in a desiccator under a fume hood for 30 min to render a hydrophobic surface.⁴ Subsequently, polydimethylsiloxane (PDMS) prepolymer (SYLGARD™ 184 Silicone Elastomer Kit) and the curing agent were mixed in a $10:1$ ratio and poured onto the master mold. The casted

PDMS was cured at 70 °C for 2 hr, then carefully peeled off, hole punched and sealed with a cover glass by oxygen plasma (Harrick Plasma). The microfluidic chips and tubing accessories were sterilized before the treatment of RBCs.

Collection of mice blood and isolation of RBCs

BALB/c mice were maintained by the Laboratory Animal Service Centre, The Chinese University of Hong Kong, Shatin, Hong Kong SAR. All animal procedures were conducted with the approval of the Animal Experimentation Ethics Committee of The Chinese University of Hong Kong (Ref No.: 18/233/MIS) and the Department of Health, the Government of the HKSAR under the Animals (Control of Experiments) Ordinance, Chapter 340 (18–522 in DH/SHS/8/2/1 Pt.12 and 18–523 in DH/SHS/8/2/1 Pt.12). For blood withdrawal, the mouse was restrained and 100 µL of blood was collected to a heparinized capillary tube from the saphenous vein by puncturing with a 25 AWG needle. The blood was washed twice with PBS by centrifugation at 500 × g for 5 min to obtain the pellet of RBCs. Expired human RBCs (HA RE001F3) were withdrawn from a 200 mL unit of packed RBCs using a 23 AWG needle in a 1 mL syringe (Becton Dickinson) and washed twice with PBS by centrifugation at 500 × g for 5 min to obtain the pellet of human RBCs. The supernatant was discarded and the isolated RBCs were diluted to a desired concentration in phosphate buffer saline (PBS) before all experiments. All investigations were conducted with freshly isolated RBCs (within 4 hr from the collection). The centrifugations were conducted at 4 °C using a high-speed refrigerated centrifuge (Neo-fuge 13 R, Heal Force).

Expression and purification of enhanced green fluorescent protein (EGFP)

EGFP was purified as described previously by hydrophobic interaction chromatography⁵. EGFP elutions were combined and dialyzed into PBS. After dialysis, protein was concentrated and used in subsequent assays. Protein concentration was measured by UV spectrometer (Eppendorf BioSpectrometer® basic, 230 V/50 – 60Hz), and protein was stored with 20% glycerol at -80 °C.

Expression and protein purification of cobalt-substituted human arginase (Co-hArgI)

pET3a-hArgI plasmid was transformed into *E.coli* BL21-Rosetta2 (DE3) expression vector and plated on the luria broth (LB) ampicillin plate⁶. Bacteria were grown in LB in the presence of 100 µg/mL ampicillin. Followed by an induction with 0.5 mM of IPTG, the bacteria were collected when the optical density measured by absorbance of 600 nm reached at 0.6. The culture was then incubated at 25 °C overnight with continuous shaking. The bacterial cells were sonicated on ice in a buffer containing 100 mM HEPES (pH 8.0), serine protease inhibitors 1 mM of phenylmethylsulfonyl fluoride and 1 mM benzamidinium-hydrochloride. Cell lysates were centrifuged, and the supernatants were filtered by a 0.22 µm filter and loaded in the Bio-Scale™ Mini Profinity™ IMAC cartridge nickel column (Biorad) for affinity chromatography. The purity of sample was determined by SDS-PAGE, and the pure hArgI elutions were combined, concentrated and dialyzed into PBS with a 10 kDa molecular weight cut-off Amicon® Ultra-15 centrifugal filter unit (Merck). In order to replace the manganese cofactor with cobalt, CoCl₂ was added to a final concentration of 10 mM in PBS and heated at 50 °C for 20 min to produce Co-hArgI⁶. The excessive CoCl₂ was dialyzed away by three rounds of buffer exchange with PBS. After dialysis, Co-hArgI was concentrated and used in subsequent assays. Protein concentration was measured by UV spectrometer (Eppendorf BioSpectrometer® basic, 230 V/50 – 60Hz) and protein was stored with 20% glycerol at -80 °C.

Labelling of Co-hArgl with fluorescent dye

Co-hArgl was labelled with Alexa Fluor™ 660 NHS Ester (Succinimidyl Ester) (Invitrogen™, catalog no. A20007) according to the manufacturer's instructions. Briefly, Co-hArgl was buffer exchanged to 0.1 M Na₂CO₃ at pH 8.5, and then mixed with Alexa Fluor™660 NHS Ester (Succinimidyl Ester) at a 1 : 10 (protein : dye) molar ratio and incubated at 25 °C for 1 hr. Afterwards, the reaction mixture was loaded onto a Bio-Gel® P-6 column with P30 resin to separate the labelled Co-hArgl from unlabeled dye. The labelled Co-hArgl (Co-hArgl-Alexa660) was then used to quantify the loading efficiency of Co-hArgl into RBCs.

Determination of hemoglobin release

The percentage of hemoglobin release was determined with an absorbance at 410 nm as previously described.⁷ Firstly, RBCs of designated amount (determined by the volume and concentration) were completely lysed by incubating the RBCs with 0.2% Triton™ X-100 in ultrapure water (Sigma Aldrich, catalog no. 9002-93-1) at 37 °C for 1 hr. The absorbance of lysed RBCs, termed as "Absorbance at total lysis", was then measured at 410 nm using the SpectraMax (Molecular Devices) micro-plate reader. For each experimental condition, the treated RBCs (the same amount as in the case of complete lysis) were centrifuged at 3000 × g for 5 min, and the supernatant was collected to detect the absorbance of released hemoglobin.

$$\text{Hemoglobin Release (\%)} = \frac{\text{Absorbance at each Experimental Conditional}}{\text{Absorbance at Total Lysis}} \times 100\% \quad (\text{S4})$$

Finally, the percentage of hemoglobin release was determined by:

Determination of preserved membrane integrity

The integrity of RBC membrane was measured by FITC-Annexin-V (BD Pharmingen™, catalog no. 556419) apoptosis assay to detect the exposure of phosphatidylserine (PS) on cell membrane.⁸ Upon membrane damage, PS would be translocated from the inner to the outer leaflet of the membrane, thus being tagged by FITC-Annexin-V. Staining was conducted according to the manufacturer's instructions. Briefly, RBCs were centrifuged and resuspended in 100 µL of binding buffer (10 mM HEPES pH 7.4, 140 mM NaCl, 2.5 mM CaCl₂). Subsequently, 5 µL of FITC-Annexin-V was added. The cells were incubated for 15 min at room temperature in the dark. The FITC-Annexin-V signal was detected by the green channel (excitation 488 nm, band pass filter: 525 ± 10 nm) using the Guava EasyCyte HT flow cytometer (Merck Millipore). Untreated RBCs were also stained and considered as the negative control. RBCs treated by different approaches were measured *via* the same settings. The portion of RBCs with PS exposure were determined by subtracting the population marked by the negative control (untreated RBCs). Finally, the percentage of preserved membrane integrity was determined by the population of intact RBCs (RBCs without PS exposure) as shown in the equation below:

$$\begin{aligned} \text{Percentage of Preserved Membrane Integrity (\%)} \\ = \text{Percentage of Intact RBCs} = (1 - \text{Portion of RBCs with PS Exposure}) \times 100\% \end{aligned} \quad (\text{S5})$$

Nonlinear fitting of hemoglobin release against shear magnitude and exposure duration

The 3D surface plot was constructed by a customized code using MATLAB 2018a and the fitting parameters were obtained by the built-in curve fitting tool in MATLAB. The nonlinear relation among the hemoglobin release (%), the flow dependent shear stress (τ) and the duration of shear exposure (T) were fitted using the power law model as described below⁹:

$$D = A\tau^\alpha T^\beta \quad (S6)$$

where, D is the percentage of hemoglobin release, and the constants A , α and β were obtained from the regression of experimental data. Fitting of the data shown in **Fig. 2B** resulted in the equation $D = 33 \times 10^{-2} \times \tau^{1.85} \times T^{0.58}$, $R^2 = 0.85$, at 95% confidence interval (CI). The fitted power function showed a close agreement with previous reports,^{10,11} particularly the contribution of shear strength and exposure duration (α and β). However, the level of hemoglobin release may be affected by the experimental setups and sample conditions, such as the membrane stiffness of RBCs and how the shear was provided.¹² Therefore, the constant in the fitted equation reported herein ($A = 33 \times 10^{-2}$) was very different from the value reported by Zhang *et al.*¹⁰ ($A = 1.228 \times 10^{-5}$), where bovine RBCs and higher shear stress (greater than 100 Pa) were employed in a Couette-type blood shearing device.

Loading of payloads to red blood cells

The isolated RBCs ($2-10 \times 10^6$ RBCs/mL) and model payloads (either EGFP or Co-hArgI) were suspended in an isotonic solution (PBS) at desired concentrations prior to the shear-mediated treatment. For each treatment, equal volume (200 μ L) of RBCs and payloads were flown through the two inlets of the microfluidic device at designated volumetric flow rates controlled by a syringe pump (PHD 2000, Harvard Apparatus). In the counter part of osmotic entrapment, the isolated RBCs were suspended in PBS at concentrations ranging from $2-10 \times 10^6$ RBCs/mL, while the model payload EGFP or Co-hArgI were suspended in a hypotonic solution (5 mM Na_2HPO_4 , pH 8.0). The RBCs and payload sample of equal volume (200 μ L) were well mixed and incubated at 37 °C for 5 min. The treated RBCs were recovered by centrifugation at $3000 \times g$ for 5 min, washed twice and resuspended in PBS prior to the subsequent investigations.

Evaluation of loading efficiency

The loading efficiency of EGFP or Co-hArgI-Alexa660 into RBCs was evaluated by the flow cytometric analysis (Guava EasyCyte HT flow cytometer, Merck Millipore). The treated RBCs were loaded into a 96-well plate (100 μ L/well), and at least 10,000 events for each condition were analyzed. The Co-hArgI-Alexa660 was excited by a 642 nm laser and the emitted signal was detected by the near infrared channel (bandpass filter: 690 ± 10 nm), whereas the EGFP was excited by a 488 nm laser and detected by the green channel (bandpass filter: 504 ± 10 nm). Fluorescently positive events were determined by subtracting the population of the negative control, where the intensities of auto-fluorescence were generated by the untreated RBCs. The loading efficiency was determined by the relative difference between the fluorescently positive events and the events of negative control. The fold increase was determined by the ratio of the measured loading efficiency or enzymatic activities between the shear-mediated loading and the osmotic entrapment.¹³ All flow cytometric data was analyzed by GuavaSoft v3.11 (Merck Millipore).

Enhanced green fluorescent protein (EGFP) gel analysis

EGFP protein or RBC-encapsulated-EGFP were loaded onto a native polyacrylamide gel without the addition of denaturant SDS. Fluorescence was detected and quantified by ChemiDoc MP imaging system (Biorad) at wavelength 488 nm.

Determination of enzymatic activity

The activities of RBC-encapsulated-Co-hArgI were determined by the colorimetric arginase assay based on the reaction of ninhydrin reagent with ornithine.^{14,15} RBC-encapsulated-Co-hArg were lysed with the assay buffer (100 mM HEPES at pH7.4) at 37 °C for 10 min to release the Co-hArg for the activity assay. The reaction was initiated by mixing the lysed RBC-encapsulated-Co-hArg to 100 mM L-arginine. After incubation at 37 °C for 3 min, the enzymatic reaction was stopped by HClO₄, followed by an addition of 20 mg/mL ninhydrin. The mixture was then heated at 95 °C for 20 min to form an orange product that was measured at an absorbance of 515 nm by a plate reader (Infinite® M1000 Pro Tecan). A standard curve was constructed by titrating the concentrations of ornithine with the same procedures as above-mentioned. The absorbance reading of RBC-encapsulated-Co-hArg was compared with the equation of standard curve to determine the amount of ornithine produced in the assay. One unit (U) of enzyme activity was defined as the amount of the enzyme producing 1 μmol of ornithine per minute at 37 °C.

Determination of cell viability

Human liver cancer (HepG2) cells were maintained in Roswell Park Memorial Institute (RPMI 1640, Thermo Fisher, catalog no. 11875119) medium supplemented with Fetal Bovine Serum (10%) (Invitrogen, catalog no. 10270-106), penicillin (100 units/mL) and streptomycin (100 μg/mL). The cells were maintained at 37 °C in a humidified incubator containing 5% CO₂. 2.5 × 10³ cells in a volume of 100 μL per well were seeded in a 96-well plate. The cells were subsequently incubated at 37 °C, 5% CO₂ overnight. Afterwards, the cells were treated with RBC-encapsulated-Co-hArgI (*n* = 3 independent experiments) and incubated for 3 days. On day 3, 10 μL of 5 mg/mL 3-(4,5-dimethyl-2-thiazoilyl)-2,5-diphenyl-2H-tetrazolium bromide (MTT) was added to each well to produce a purple insoluble product. Two hours later, the supernatant was aspirated and 100 μL of DMSO was added to each well. The change in color intensity was measured at an absorbance 565 nm by a plate reader (Infinite® M1000 Pro Tecan). The cell viability was normalized against the absorbance value of the negative control as shown below:

$$\text{Cell Viability} = \frac{\text{Absorbance of (RBC - Encapsulated Co - hArgI) Incubated with HepG2 Cells}}{\text{Absorbance of (Untreated RBCs) Incubated with HepG2 Cells}} \times 100\% \quad (S7)$$

Measurement of deformation index (DI)

The deformability of treated RBCs were measured following the previously reported procedures.¹⁶ A calibration plot was obtained by measuring the deformation index (DI) of RBCs at varied shear stress. ⁹ESI Fig. S8 showed that the DI reached a plateau at a shear stress ≥ 20 Pa for the mouse RBCs. Therefore, a shear stress of 20 Pa was applied to measure the DI of treated RBCs. The RBCs were visualized by a high-speed camera (Dimax CS3, PCO AG, Kelheim) in a frame rate ranged from 8,000 to 10,000 frames per second at the shutter exposure of 1 μs. The captured frames were processed with Advanced Research v5.01 (NIS Elements, Nikon Incorporation). The DI was quantified by ImageJ v1.8 (NIH) according to the Taylor's estimation on object's small deformation as shown in the equation below¹⁷:

$$DI = \frac{L - b}{L + b} \quad (S8)$$

where, L and b represent the lengths of the major axis and the minor axis of ellipsoidal shape of the deformed RBCs.

Scanning electron microscopy (SEM) imaging

The treated RBCs were centrifuged and resuspended in 2.5% glutaraldehyde in PBS for fixation at 4 °C overnight. The fixed cells were centrifuged and washed with PBS three times. The RBCs were then dehydrated with a gradient increase of ethanol solutions (30, 50, 70, 90 and 100 %) for three times and incubated with hexamethyldisilazane (HMDS) (Sigma Aldrich, catalog no. H4875) for 15 min twice. The RBCs in HMDS were resuspended and loaded on the coverslips and air-dried. Finally, the coverslips were coated with Pt/Au and subjected to scanning electron microscopy (Prisma™ E SEM, Thermo Fisher Scientific) imaging at the voltage between 5-10 kV. To obtain the electron micrographs of the close-up view of the cross-section, PDMS channel surface was coated with Pt/Au and subjected to scanning electron microscopy imaging.

Statistical analysis

At least three independent experiments were analyzed for each data set unless otherwise specified. The results were plotted as mean \pm standard deviation (SD). The statistical significance was determined by two-tailed unpaired student's t-test with 95% confidence level using Graphpad Prism v.8.

ESI Fig.

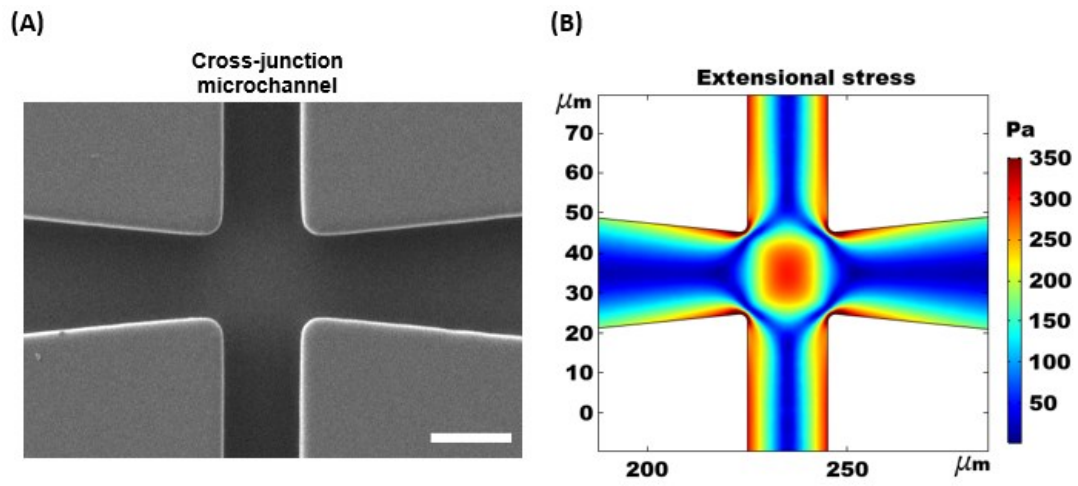


Fig. S1. (A) Scanning electron microscopy image at the cross-junction of the designed microchannel for the transient deformation of RBCs. The entire microfluidic channel has a uniform depth of 40 μm . Scale bar: 20 μm . (B) Extensional stress distribution surrounding the stagnation point at the cross-junction.

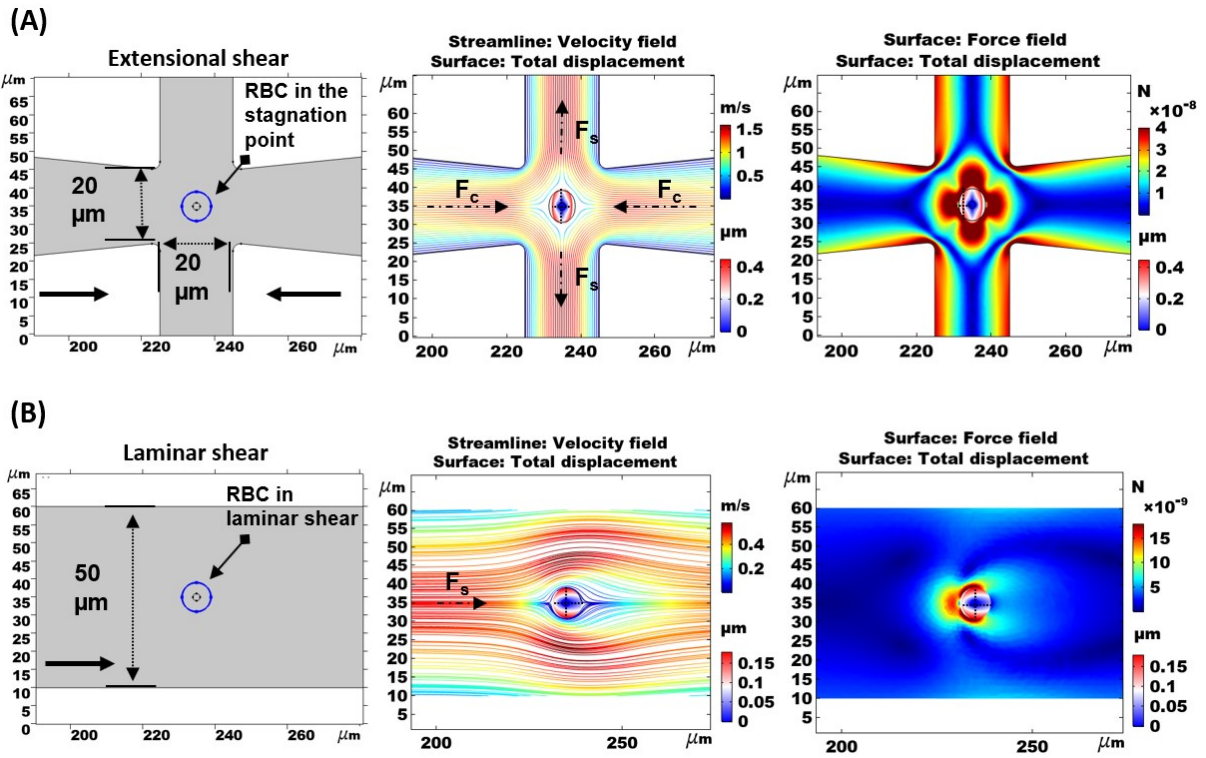


Fig. S2: Comparison of the deformation of RBCs under **(A)** extensional shear at the cross-junction and **(B)** steady laminar shear in a straight channel. The channel geometry (blue circle showed the fluid-structure interaction boundary), velocity streamlines and force field were illustrated in the left, central and right panel, respectively. Surrounding the stagnation point of the extensional shear produced the compression force (F_c) acting normally on the cell surface and the laminar shear force (F_s) acting along the direction of flow. Dotted line on the force field illustrated the major and minor axis of ellipsoidal deformed RBCs.

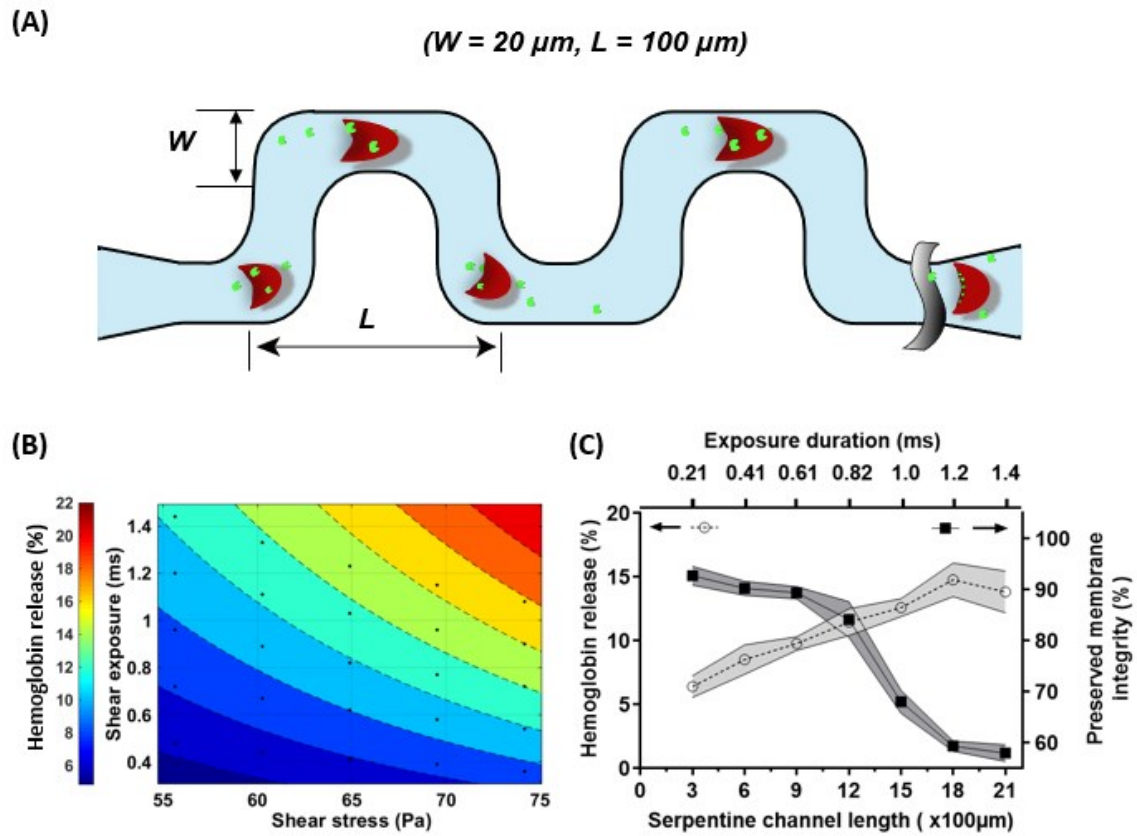


Fig. S3. (A) Geometry of the serpentine microchannel and the schematic showing the extended deformation of RBCs modulated by the length of serpentine channel. (B) Heat map denotes the combinatorial effect of shear stress and duration of shear exposure to the percentage of hemoglobin release. (C) Effect of the duration of shear exposure to the hemoglobin release at a constant shear stress (64.9 Pa). The shaded areas surrounding the dotted line showed mean \pm SD ($n = 3$ independent experiments using the same batch of mouse RBCs).

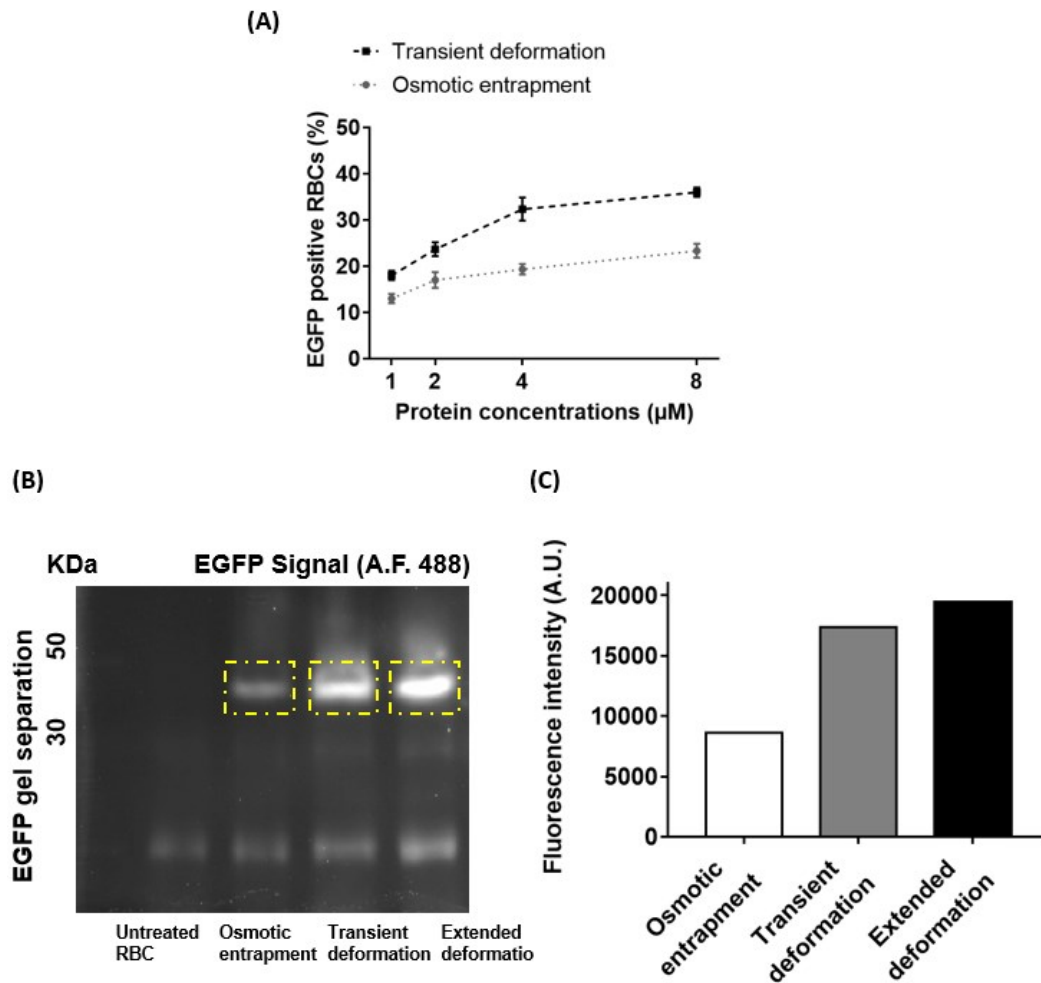


Fig. S4. (A) Effect of protein concentrations to the loading efficiency at a constant concentration of RBCs (4×10^6 cells/mL). Results were plotted as mean \pm SD ($n = 3$ independent experiments). **(B)** A native polyacrylamide gel illuminated by an excitation of 488 nm showing the EGFP band after lysis of RBCs treated by the three approaches. The untreated RBCs served as the negative control. **(C)** Fluorescent intensity of the corresponding EGFP bands [yellow dotted boxes in **(B)**].

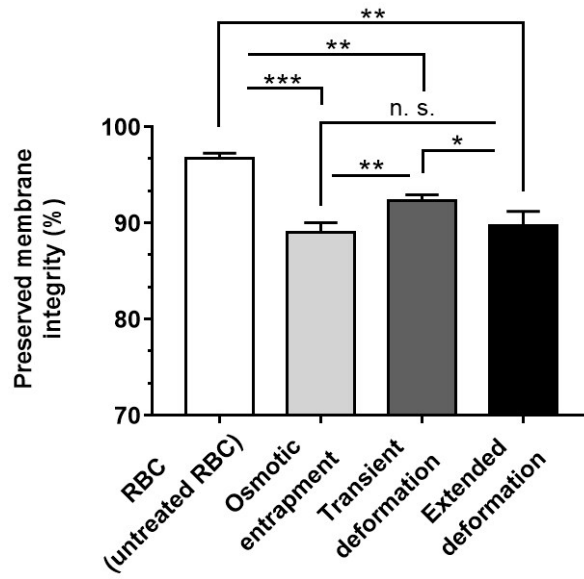


Fig. S5. Preserved membrane integrity of treated RBCs measured immediately after the treatments. Results were plotted as mean \pm SD ($n = 3$ independent experiments * $p < 0.05$, ** $p < 0.01$, *** $p < 0.001$, n.s.: not significant).

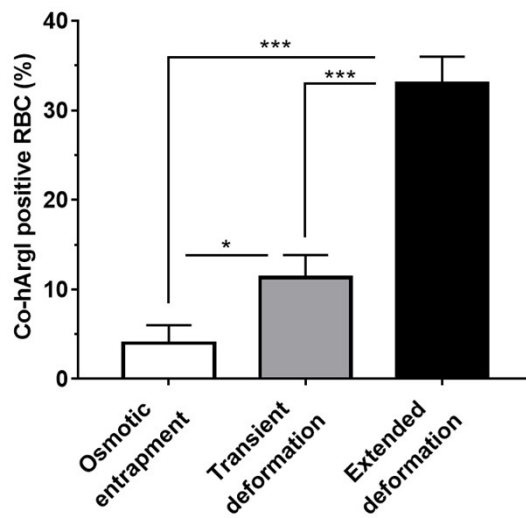


Fig. S6. Loading of fluorescently labelled (Alexa Fluor™ 660 NHS Ester) Co-hArgI into mouse RBCs. Results were plotted as mean \pm SD ($n = 3$ independent experiments, * $p < 0.05$, *** $p < 0.001$).

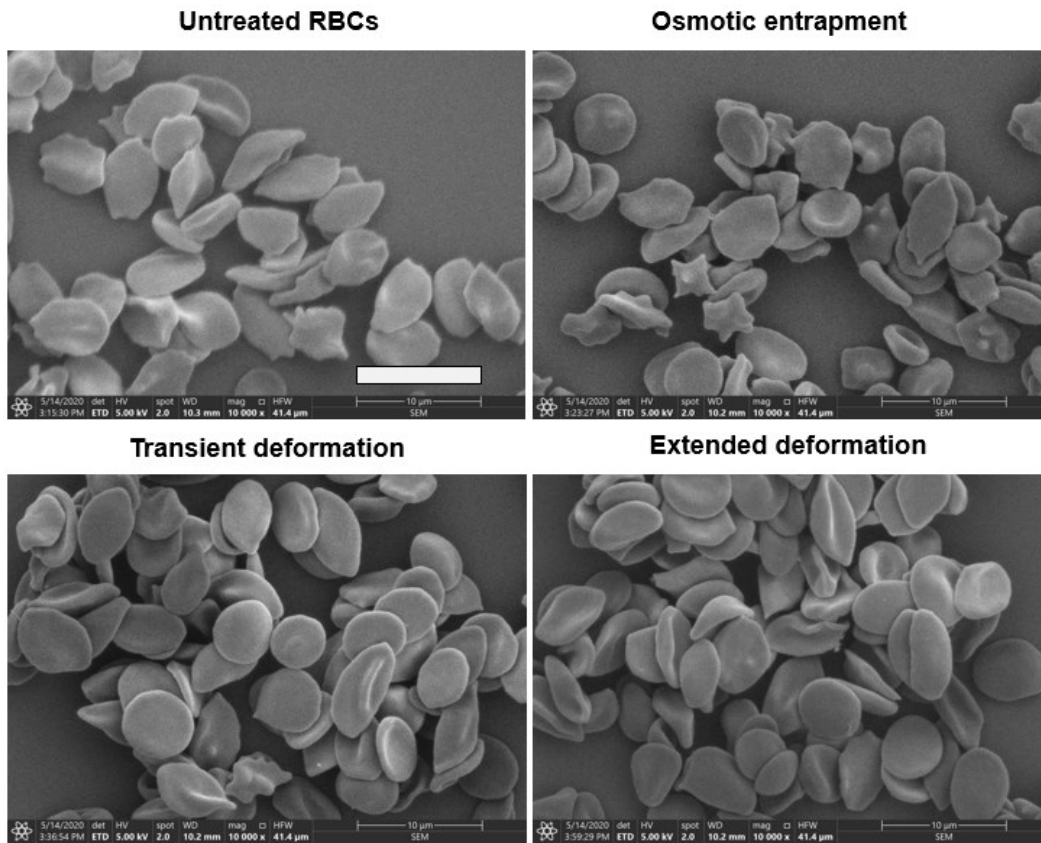


Fig. S7. Morphologies of treated RBCs using different approaches as observed under SEM. Scale bar: 10 μm.

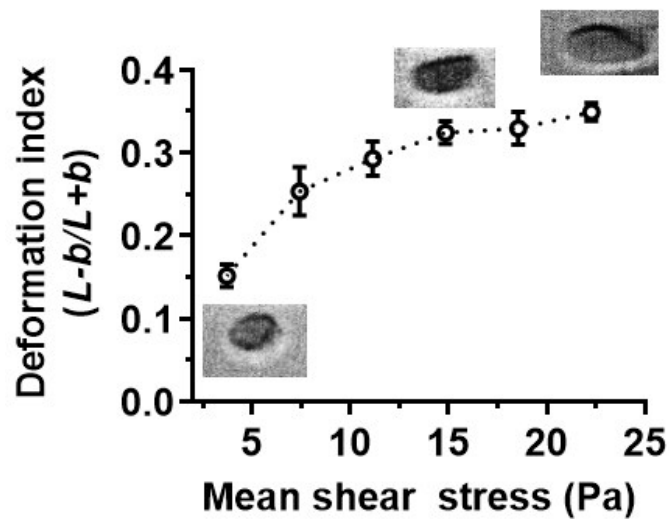


Fig. S8. Deformability index (DI) measured under different mean shear stress in the constricted microchannel. Insets showed representative images of deformed RBCs at the corresponding shear stress. Results were plotted as mean \pm SD ($n = 10$ RBCs for each condition).

References:

- 1 I. Dulińska, M. Targosz, W. Strojny, M. Lekka, P. Czuba, W. Balwierz and M. Szymoński, *J. Biochem. Biophys. Methods*, 2006, **66**, 1–11.
- 2 O. C. Zienkiewicz, R. L. Taylor and P. Nithiarasu, *The Finite Element Method for Fluid Dynamics*, Elsevier, Waltham, 7th edn., 2014.
- 3 E. N. L. R. Byron Bird, Warren E. Stewart, *Transport Phenomena*, John Wiley and Sons, New York, 2nd edn., 2007.
- 4 D. Qin, Y. Xia and G. M. Whitesides, *Nat. Protoc.*, 2010, **5**, 491–502.
- 5 J. R. Deschamps, C. E. Miller and K. B. Ward, *Protein Expr. Purif.*, 1995, **6**, 555–558.
- 6 E. M. Stone, V. S. Glazer, L. Chantranupong, P. Cherukuri, R. M. Breece, D. L. Tierney, S. A. Curley, B. L. Iverson and G. Georgiou, *ACS Chem. Biol.*, 2010, **5**, 333–342.
- 7 Y. M. Kwon, H. S. Chung, C. Moon, J. Yockman, Y. J. Park, S. D. Gitlin, A. E. David and V. C. Yang, *J. Control. Release*, 2009, **139**, 182–189.
- 8 R. Huisjes, A. Bogdanova, W. W. Solinge, R. M. Schiffelers, L. Kaestner and R. Wijk, *Front. Physiol.*, 2018, **9**, No. 656.
- 9 M. Giersiepen, L. J. Wurzinger, R. Opitz and H. Reul, *Int. J. Artif. Organs*, 1990, **13**, 300–306.
- 10 T. Zhang, M. E. Taskin, H. Bin Fang, A. Pampori, R. Jarvik, B. P. Griffith and Z. J. Wu, *Artif. Organs*, 2012, **35**, 1180–1186.
- 11 R. Paul, J. Apel, S. Klaus, F. Schügner, P. Schwindke and H. Reul, *Artif. Organs*, 2003, **27**, 517–529.
- 12 G. Casagrande, F. Arienti, A. Mazzocchi, F. Taverna, F. Ravagnani and M. L. Costantino, *Artif. Organs*, 2016, **40**, 959–970.
- 13 M. Cieńska, K. Labus, M. Lewańczuk, T. Koźlecki, J. Liesiene and J. Bryjak, *PLoS One*, 2016, **11**, No. e0164213.
- 14 E. W. Iyamu, T. Asakura and G. M. Woods, *Anal. Biochem.*, 2008, **383**, 332–334.
- 15 F. P. Chinard, *J. Biol. Chem.*, 1952, **199**, 91–95.
- 16 Y. Zheng, J. Chen, T. Cui, N. Shehata, C. Wang and Y. Sun, *Lab Chip*, 2014, **14**, 577–583.
- 17 G. I. Taylor, *Proc. R. Soc. A Math. Phys. Eng. Sci.*, 1934, **146**, 501–523.